photonics

MDPI

Communication

Optical Detection of VOC Vapors Using Nb_2O_5 Bragg Stack in Transmission Mode

Rosen Georgiev *, Yoana Chorbadzhiyska, Venelin Pavlov, Biliana Georgieva and Tsvetanka Babeva

Institute of Optical Materials and Technologies "Acad. J. Malinowski", Bulgarian Academy of Sciences, Akad. G. Bonchev str., bl. 109, 1113 Sofia, Bulgaria; yoanach@iomt.bas.bg (Y.C.); venelinp@iomt.bas.bg (V.P.); biliana@iomt.bas.bg (B.G.); babeva@iomt.bas.bg (T.B.)

* Correspondence: rgeorgiev@iomt.bas.bg

Abstract: In this study, an emphasis is put on vapor-sensitive Bragg stacks as an important class of optical sensors. All-niobia Bragg stacks were deposited by spin-coating of sol-gel Nb_2O_5 thin films alternated with mesoporous layers after proper design through optimization of operating wavelength and number of layers in the stack. Mesoporous Nb_2O_5 films with different morphology and identical structure were obtained using organic templates (Pluronics PE6200 and PE6800) and subsequent annealing. Transmittance measurements were performed as a detection method that offers technological simplicity and accuracy. It was demonstrated that stacks including PE6200 templated films exhibit higher sensitivity than stacks templated with PE6800. It was assumed and verified by computer-aided modelling of experimental data that mesoporous films prepared with addition of PE6200, although less porous, were more stable compared to those templated with PE6800, and did not collapse during the thermal treatment of the stacks. Furthermore, the reproducibility of optical response was studied by sorption and desorption cycles of acetone vapors. The suitability of all-niobia Bragg stacks for optical sensing of VOCs was discussed.

Keywords: optical sensing; Bragg stacks; Nb_2O_5; mesoporous films; sol-gel

Citation: Georgiev, R.; Chorbadzhiyska, Y.; Pavlov, V.; Georgieva, B.; Babeva, T. Optical Detection of VOC Vapors Using Nb_2O_5 Bragg Stack in Transmission Mode. *Photonics* **2021**, *8*, 399. https://doi.org/10.3390/photonics8090399

Received: 30 August 2021
Accepted: 16 September 2021
Published: 18 September 2021

1. Introduction

Conventional Bragg stacks are structures that consist of alternatingly deposited two materials having low and high refractive indices and quarter-wavelength optical thickness, which allow constructive and destructive interference of multiple reflected and transmitted light waves, respectively, thus engineering a photonic band gap of high reflectance and low transmittance of photons of particular energy. Those structures have been a focus of research due to their ability to control the propagation of light in various ways [1–3] revealing their vast versatility and applicability. To date, a plethora of materials [4] has been tested in order to achieve precise control of the structure parameters, and still the optimum spot between durability, tunability, and effectiveness of optical response is an open question.

The most common approach in inorganic vapor sensitive Bragg stack deposition is the inclusion of mesoporous material layers, which are inherently extremely sensitive to the environment changes due to their unique properties such as controllable pore size [5,6] and enhanced surface area [7]. Indeed, their inclusion in Bragg stacks could be used for modification of their effective refractive index caused by external stimuli such as vapors or liquids, resulting in change of the structure band gap and color.

Mesoporous materials are now relatively easy to fabricate in various ways [8]. However, the need of media with contrast in refractive index value to create Bragg stacks brings to the forefront the need of coating technology for more different materials. The manufacturing cost, compatibility, and materials quality are other factors that limit the materials of choice. To the best of our knowledge the most common combination reported in the literature is TiO_2/SiO_2, which is, however, challenging itself due to the considerable shrinkage during the condensation reaction, polymer removal, and titania crystallization, which typically leads to crack formation and delamination [9]. Crack formation is also to be considered due to lattice mismatch of the adjacent interfaces during thermal treatment and coating formation.

Nb_2O_5 is well a studied material with wide application in energy storage [10,11] and optoelectronics [12] due to its chemical resistivity, high refractive index value, and aging durability. Previously, our group has studied the optical parameters of mesoporous Nb_2O_5 thin films mesostructured with different organic templates and concentrations in order to achieve reproducible film parameters [13,14]. A single layer reaction has been quantified when exposed to acetone vapors and Bragg stack of one material in two different forms (dense and porous) has been successfully deposited and used as a sensing medium for VOC's detection using reflectance measurements. Thus, we have managed to overcome some of the challenges related to those structures.

In this study, we continue our previous work in the direction of enhancing the sensitivity of all-niobia Bragg stacks. The sensing measurements are performed in transmission mode that is linked with easier technological set-up, higher sensing reaction and wider applicability for future photonics. Bragg stacks of dense and porous Nb_2O_5 films were properly designed by optimization of operating wavelength and number of layers in the stack, and then were experimentally realized. In order to study the influence of films morphology on sensing behavior and sensitivity of the stack, two different mesoporous films, templated with commercially available triblock co-polymers PE6200 and PE6800, were implemented as low refractive index medium in the stacks. The sensitivity, stability, and reproducibility of the structures were studied and discussed.

2. Materials and Methods

For the preparation of Bragg stacks, two types of Nb_2O_5 thin films were used—dense and porous. They were prepared by a combination of sol-gel and spin coating methods. Niobium sol was synthesized following recipe [15] starting from niobium chloride as a precursor: 400 mg niobium chloride (99%, Sigma-Aldrich, St. Louis, MO, USA) was added to 0.6 mL of ethanol and then placed in ultrasonic bath for 30 min. The resulting mixture was added to 0.17 mL of distilled water and 3 mL of ethanol, the process of ultrasonic treatment was then repeated. In the last step, 4.7 mL ethanol was added, achieving the desired concentration of niobium precursor for deposition of thin layers in clear solution. Porosity was introduced by evaporation self-assembly with two commercially available organic templates—Pluronic PE6200 and PE6800 (BASF). Aqueous polymers solutions with concentrations of 20 wt% were added to the sol in 1:5 volume ratios shortly before deposition. Thin films were deposited by spin coating at 4000 rpm for 60 s. Final film composition was obtained by annealing at 320 °C for 30 min.

Single-layer optical characterization was carried out with UV-VIS-NIR spectrophotometer Cary 05E (Agilent, Santa Clara, CA 95051, USA). Optical constants and thicknesses of the films were calculated by nonlinear curve fitting method out of the reflection spectra of the films measured in spectral range between 320 nm and 900 nm. Refractive indices were further used for porosity determination by Bruggemann effective medium approximation [16]. Morphological and structural features of the films were inspected by Transmission Electron Microscopy (TEM) and Selected Area Electron Diffraction (SAED), respectively using HRTEM JEOL JEM 2100 (Tokyo, Japan) microscope. The samples for TEM analysis were prepared by the same procedure mentioned above, but on monocrystal NaCl substrate. Films were removed by resolving the substrate in distilled water and transferred on standard copper grids. After drying at ambient conditions for 24 h, the samples were ready for direct observation in TEM.

The preparation of 7-layer Bragg stacks was performed onto fused silica substrates by alternating deposition of dense and porous niobia films, starting from the dense one, using spin coating (4000 rpm, 60 s). After each layer deposition, the samples were heated to 320 °C (5 °C/min) without holding the temperature in order to form layers' interfaces.

After the 7th layer deposition, the structure was thermally treated for 30 min at 320 °C for final template removal.

The sensing response was studied toward acetone vapors as probe molecules in home-made bubbler for generation of vapors from liquids with controlled concentrations. The experimental set-up is described in detail elsewhere [17]. Briefly, the vapor sensing measurements were implemented in a Cary 05E spectrophotometer equipped with quartz cell with gas inlet and outlet and a homemade bubbler system for generation of vapors from liquids. Argon was used as a carrier gas, both for bubbling through liquid acetone in the saturator and for desorption measurements. The saturator was thermally isolated and kept at constant temperature of 0 °C. The relative pressure p/p_0 =0.15 (p_0 pressure of saturated vapors at 0 °C) was achieved by flowmeters, valves, and a mixing chamber. The sample was placed in the quartz cell, and the ambient was cycled between acetone vapors (sorption measurements) and argon (desorption measurements). Transmittance spectra of the structure were measured in both atmospheres, i.e., prior to (T_{Ar}) and during vapor exposure (T_{Ac}), and the difference $\Delta T_{\max} = T_{\mathrm{Ar}} - T_{\mathrm{Ac}}$ was recorded. The values of $\Delta T_{\max}$ were considered as the sensitivity of the samples, and they were used to compare the optical response of studied media.

3. Results and Discussion

3.1. Morphology and Structure of Single Layers

The morphology of films was studied by TEM, while their amorphous structure was confirmed by SAED. The comparison between dense films, i.e., Nb_2O_5 films prepared without a template, and mesoporous films mp-niobia-PE6200 and mp-niobia-PE6800 templated with commercially available triblock co-polymers Pluronic PE6200 and PE6800, respectively, is presented in Figure 1. Dense Nb_2O_5 film has a smooth surface without any specific features, and exhibits microporosity that is typical for chemically deposited materials. On the other hand, it is seen from Figure 1b,c,e,f that the organic template has great influence on the morphology of the films. Firstly, the addition of template results in developed surface area and a presence of pores which are arranged in non-periodic manner and ranging in size between 5 and 10 nm, thus classifying the materials as mesoporous. Secondly, the two different types of organic templates lead to formation of differently shaped pores. When PE6800 is implemented as a template, almost spherical pores with similar sizes are created (Figure 1c,f). However, in the case of PE6200, pores are arranged in rows with different lengths which are randomly oriented. At selected annealing conditions (320 °C, 30 min) both dense and porous films are amorphous (verified by SAED) and crack-free.

3.2. Optical and Sensing Properties of Single Films

Refractive index (*n*), extinction coefficient (*k*), and thickness (*d*) of single thin films deposited on silicon substrates were calculated using previously developed procedures described in detail elsewhere [15]. Briefly, goal function comprising discrepancies between measured and calculated reflectance spectra was minimized using non-linear curve fitting methods through the variation of six parameters that are constants with respect to wavelength. These are film thickness and five constants of the dispersion equations used for describing spectral dependences of *n* and *k*. For initial values of the fitting parameters, we used a 6-dimensional mesh, ran the minimization at each point of the mesh, and calculated the fitting error. In the next step, the size of the mesh is reduced by selection of area with the smallest error, and the fitting is run again. This procedure is repeated until the fitting error stops changing. The solution with the smallest fitting error is selected as a true one.

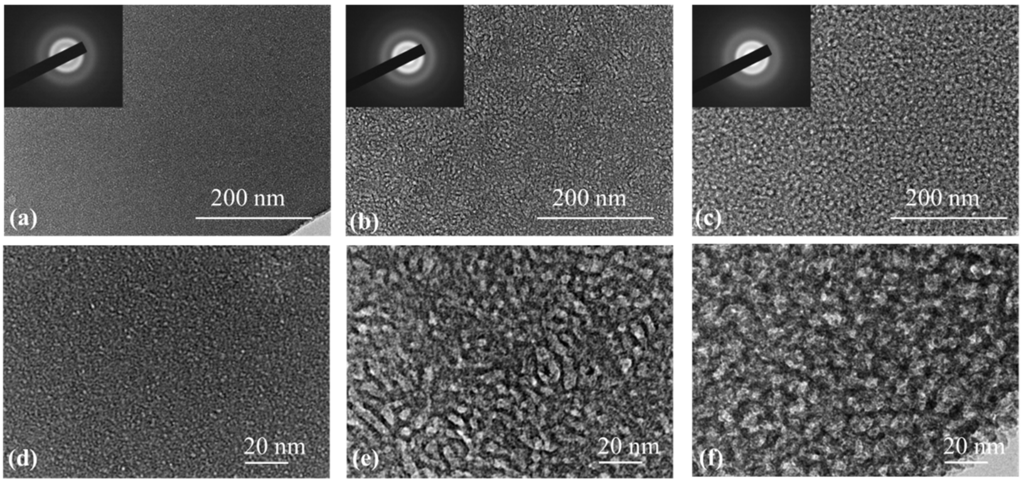

Figure 1. TEM images and corresponding SAED patterns (as insets) of dense Nb_2O_5 thin films (**a**,**d**) and Nb_2O_5 films templated with aqueous solutions of Pluronic PE 6200 (**b**,**e**) and Pluronic PE 6800 (**c**,**f**) with concentration of 20% w/v.

The calculated values of refractive index of the films are presented in Figure 2. As it is expected, the templated films exhibit lower refractive index as compared to the dense one. The impact of different pore morphology on refractive index of porous films is well seen in Figure 2: the smaller refractive index and higher porosity is achieved in the case of spherical pores (porous film templated with PE6800). Although the free volume fraction in PE6800-templated films is higher as compared to this in PE6200 templated films (50% and 35%, respectively), the change in refractive index Δn of single films due to exposure to acetone vapors is slightly higher in PE6200 templated films (0.035) [14] as compared to Δn for PE6800-templated one (0.028) [18]. This means that absorption, penetration, and condensation of vapors are more effective when pores are arranged in rows than when they are randomly scattered in the film.

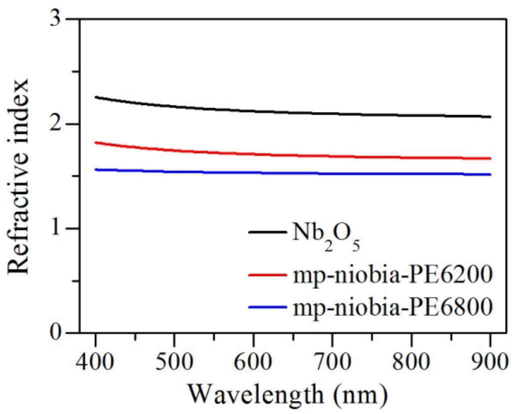

Figure 2. Dispersion curves of dense and porous Nb_2O_5 after annealing at 320 °C for 30 min.

It is well known that one possible approach for increasing the optical sensing response is to incorporate the sensitive thin film in quarter-wavelength multilayer structure, referred to as Bragg stack. We have already experimentally achieved a more than 10 times increase in sensitivity using 7-layers Bragg stack in reflectance mode [19]. Usually, detection in transmission mode is preferred, as measuring the transmitted light is simpler, more accurate, and cheaper as compared to measuring reflected intensity. Furthermore transmittance can be measured at normal light incidence that overcomes the complications related to polarization effects and incident angle dependences. In the ideal case of zero absorption in the films, the changes in reflectance $\Delta R_{\max}$ and transmittance $\Delta T_{\max}$ of the stack due to change of n (Δn) and/or d (Δd) of the films are the same. However, in the real case, the absorption of the film, although very small, is still not zero. This leads to smaller change of $\Delta T_{\max}$ as compared to $\Delta R_{\max}$ at the same Δn and/or Δd. Therefore, the proper design of a Bragg stack is essential in order to obtain the highest possible value of $\Delta T_{\max}$.

3.3. Design of Bragg Stacks

3.3.1. Selection of Optimal Number of Layers in the Stack

The starting point of Bragg stack design was to determine the optimal number of layers, N. This is of utmost importance to determine the trade-off between the efforts to build the structure and the expected sensing response. Generally, the more layers in the stack, the greater the sensitivity as the number of layers increases the stop band becomes more and more efficient. This is illustrated in Figure 3a which presents the calculated stop bands of modeled stacks built of different numbers of layers.

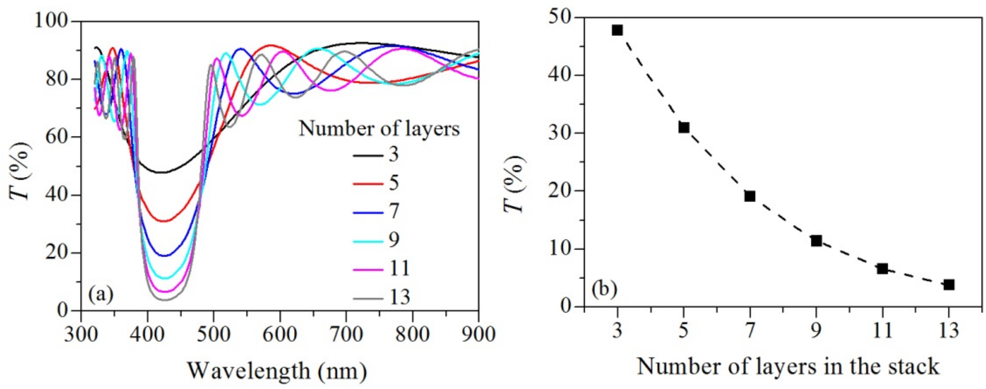

Figure 3. Transmittance spectra of modeled Bragg stacks (**a**) and stop band intensity as a function of number of the layers in the stacks (**b**).

It is obvious that the slope of the edges determines the sensitivity, as when the stop band shifts, due to a change of effective refractive index, for example, the change in T at a fixed wavelength will be stronger when the edge's slope is higher. However, in a real case two issues should be considered. The first is related to the vapor penetration. With increasing the number of the layers in the stack, the diffusion path also increases, and the vapors may not reach all layers in the stack. As a result, only some of them will contribute to $\Delta T_{\max}$ and the overall change in T will be smaller as compared to when the refractive indices of all porous layers change due to vapor exposure. The second issue that should be accounted for is the unavoidable deviation from the target thickness that accumulates with the number of layers in the stack and results in the deterioration of the already created band gap. Hence, an acceptable compromise should be made when selecting the optimal number of layers in the stack.

It is clear from Figure 3a that when the slope of the band increases, the intensity of the stop band decreases. Figure 3b presents the stop band intensity (T at the center of the stop band) as a function of the number of layers in the stacks, N. There is a substantial decrease in T when N is changing from 3 to 7, whereafter the reduction in T becomes smaller. A similar trend is observed for the dependence of band slopes on N. Thus, a conclusion could be derived that a 7-layer Bragg stack is an acceptable choice in the viewpoint of maximum sensitivity and minimum deposition inaccuracies.

3.3.2. Selection of the Spectral Position of Stop Band

The next step of our investigation was to check whether the stack sensitivity depends on the band gap spectral position. As the sensing will be in transmission mode, we modelled 7-layer stacks with stop bands at different spectral positions in the range of 400–600 nm, and calculated the change in the transmission spectrum of different Bragg stacks when exposed to acetone vapors. As we know that vapor exposure only influences the refractive index of the porous films, the spectra after exposure were modelled by increasing n of all porous films in the stack by 0.03. The calculated values of ΔT_{max} as a function of central wavelength of the stop band are plotted in Figure 4. It is seen that, in order to achieve the greatest sensitivity, Bragg stacks with stop bands in the range from 415 nm to 450 nm need to be designed.

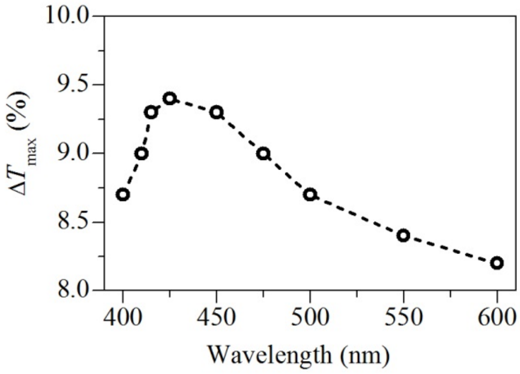

Figure 4. Calculated changes of transmittance of 7-layer Bragg stacks comprising of dense and porous Nb_2O_5 layers having stop bands at different wavelengths when refractive index of all porous layers increases by 0.03.

3.4. Sensing of Acetone Vapors

In the next step of our investigation, we deposited 7-layer stacks consisting of dense and porous Nb_2O_5 as high and low refractive index media, respectively. Porous Nb_2O_5 was obtained using two organic templates: Pluronic PE6200 and Pluronic PE6800. The operation wavelength (λ_c) of both stacks was selected to be 440 nm, as this is the wavelength at which the highest sensitivity is expected (see Figure 4). By means of refractive index values of single films, we calculated the target thicknesses of the layers in the stacks using the Bragg equation $n_H \cdot d_H = n_L \cdot d_L = \lambda_c/4$, where n_H and n_L are refractive indices of dense and porous films, respectively. Thus, the target value for thickness of dense layer d_H was 50 nm for both stacks, while the targeted thicknesses d_L of porous layers were 62 nm and 71 nm for PE6200 and PE6800 templated layers, respectively. We used these structures for the detection of vapors of volatile organic compounds with an optical read-out in transmission mode. In the typical experiment, the stack was placed in a transparent cell located in the compartment of the spectrophotometer, and the atmosphere in the cell was varied from argon to acetone vapors. The two spectra taken at the same spot of the sample in argon and acetone ambient are shown in Figure 5a for stack templated with PE6800, and in Figure 5b for the one prepared using PE6200 as organic template.

As the acetone vapors condense in the pores of mesoporous films, and replace the air inside with acetone with a higher refractive index, the effective refractive index of the mesoporous layers increases, thus decreasing the optical contrast of the stack. This leads to red shift of the stop band mostly pronounced for its short-wavelength edge. The shift is stronger for the stack with PE6200 templated layers. The change of transmittance ΔT_{max} is 10.9% for mp-niobia-PE6200 containing stack, and 6.3% for the stack including porous films templated with PE6800. This means that the change in the effective refractive index of mp-niobia-PE6200 is higher compared to mp-niobia-PE6800, which is in accordance with the results obtained for sensing response of single porous films (Δn_{Ac} is 0.028 [18] and 0.035 [14] for PE6800 and PE6200 templated stacks). The comparison between Figure 5a,b shows that the stop band of stack including mp-niobia-PE6200 films is wider as compared to that in PE6800 templated stack indicating higher optical contrast in the first case. However, this contradicts the results obtained for the single films showing that refractive index of mp-niobia-PE6800 is less than that of mp-niobia-PE6200. As the optical contrast in the first case is higher, it should be expected that the stop band will also be wider. An assumption could be made that, for some reason, the refractive index of mp-niobia-PE6800 film in the stack is higher compared to that of single film. Keeping in mind that the refractive index is proportional to density, we may further assume that mp-niobia-PE6800s in the stack are denser, i.e., less porous, compared to single films. This could explain the smaller vapor response of the stack, including mp-niobia-PE6800, as lower porosity leads to penetration difficulties and is responsible for less effective absorption in this film.

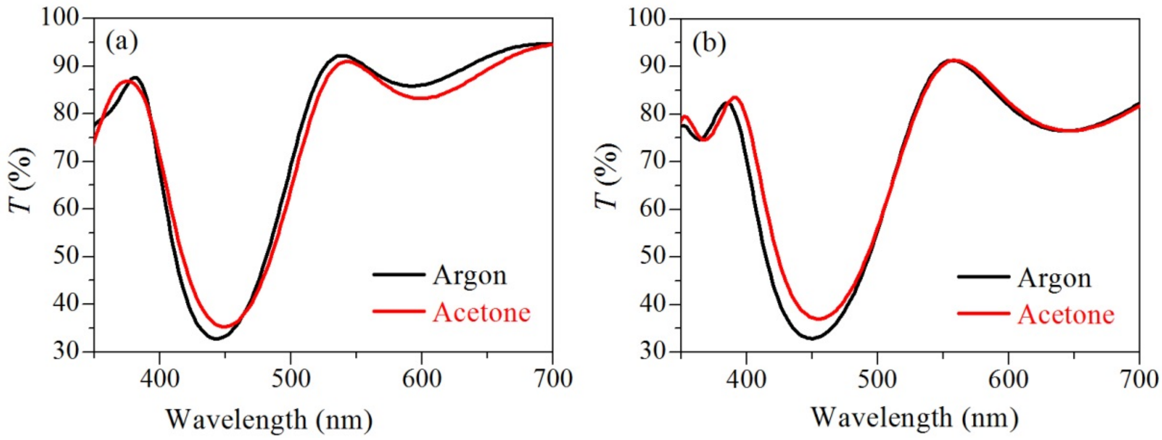

Figure 5. Measured transmission spectra in argon and acetone ambient of 7-layer Bragg stacks, deposited by alternating dense and porous Nb_2O_5 layers, structured by Pluronic PE6800 (**a**) and PE6200 (**b**) as templates.

In order to verify these assumptions, we have determined the thicknesses of the layers in the stacks and their refractive indices through curve fitting of the measured transmittance spectra of the stacks. Refractive indices of single films, along with calculated target thicknesses, were used as initial values in the fitting. The results obtained in the case of PE6200 for measured and calculated spectra in argon and acetone are presented in Figure 6a. Similar results were obtained for stack comprising mp-niobia-PE6800 as low-*n* medium.

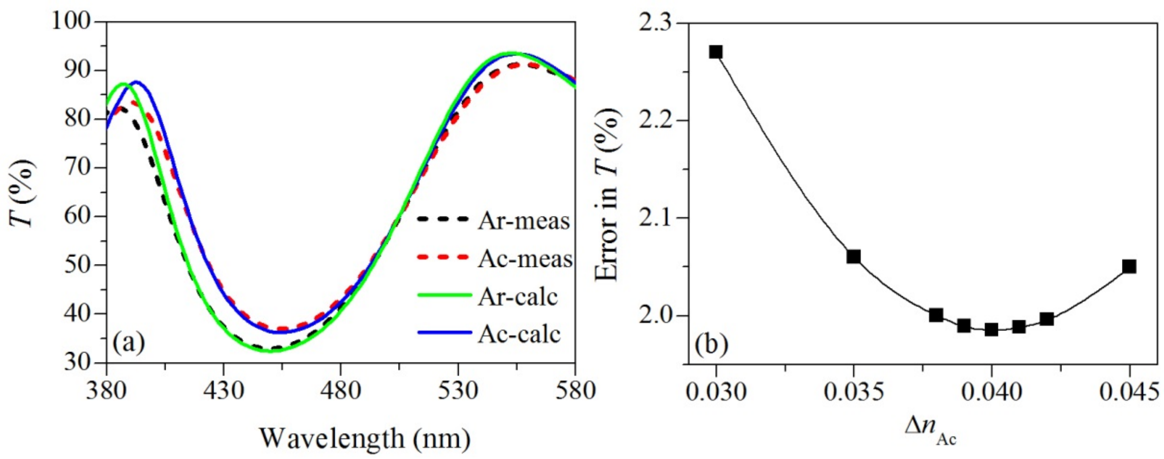

Figure 6. (**a**) Calculated and measured transmittance spectra of 7-layer stacks consisting of dense Nb_2O_5 as high refractive index medium and mesoporous Nb_2O_5 obtained using Pluronic PE6200 as a low refractive index medium in argon and acetone ambient; (**b**) Dependence of fitting error on refractive index change Δn_{Ac} generated by acetone vapor condensation.

In the case of PE6200, the best match was obtained with layer thicknesses of 53 nm/67.9 nm/48 nm/62.4 nm/50.5 nm/62.9 nm/48.1 nm, where the first value is for the layer closest to the substrate. The obtained values of d_H are very close to the target value of 50 nm, with average deviation of 0.1 nm. Except for the first porous layer, a good match between target (62 nm) and real d_L is obtained for mp-niobia-PE6200, as well with average deviation of 2.4 nm. According to the calculated refractive indices of both dense and porous films, n_H matches n of single film, while n_L of mp-niobia-PE6200 in the stack is slightly higher as compared to the refractive index of single film: 1.83 and 1.77, respectively, at wavelength of 440 nm.

In the case of PE6800, the results of curve fitting for the stack's thicknesses are 48 nm/51.6 nm/52 nm/68.5 nm/52 nm/58.4 nm/48 nm. Similarly, the average thickness deviation of dense films in the stack from target value of 50 nm is negligible. However, a substantial reduction in porous layer thickness is observed, with an average deviation of 11.5 nm from the target value of 71 nm. The reduction is most pronounced for the mp-niobia-PE6800 layer which is closest to the substrate: the calculated thickness is 51.6 nm. Simultaneously, the calculations indicate that mp-niobia-PE6800 films in the stack have notably higher refractive index as compared to single films: n_L at wavelength of 440 nm is 1.86, thus an increase of 0.31 is obtained. The observed reduction in thickness of porous films accompanied with substantial increase in refractive index confirmed the assumption made above that the porosity of mp-niobia-PE6800 significantly decreases when film is incorporated in the stack. The calculated free volumes using the Bruggemann effective medium approach [16] are 50% of single film and 23% after incorporation of the same film in the Bragg stack, thus verifying the reduction in porosity. The most probable reason is the multiple heating of the stack that leads to collapse of the thin pores' walls of PE6800-tempated film. In contrast, the porosity of mp-niobia-PE6200 film in the stack is almost unaffected by similar annealing: the porosity of the single films is 35% and slightly decreases to 30% after incorporation of the films in the stack. The possible explanation is the different intrinsic porosity of both porous films. In the case of the PE6800, template, the porosity is 50%, presupposing thin walls of the pores and an unstable film skeleton that easily collapses when subjected to prolonged heating. It is realistic to assume that smaller free volume fractions of PE6200 templated film (35%) along with a different morphology (pores arranged in rows) result in more rigid and stable skeleton that stands the applied thermal treatment.

The change of the refractive index (Δn_{Ac}) of porous films due to condensation of acetone in the pores was obtained through the fitting of transmittance spectra measured in acetone ambient. In calculations of Δn_{Ac}, the thicknesses of the layers in the stack were set as known parameters equal to the thickness values obtained for argon, while the refractive index of all porous layers in the stack was increased gradually, until the fitting error reaches its minimum (Figure 6b). The calculations demonstrate that, due to acetone vapor exposure, the effective refractive index increased by 0.040 and 0.011 for each porous layer of the stacks templated with PE6200 and PE6800, respectively. Taking into consideration the collapse observed for mp-niobia-PE6800 films, this result is expected. Considering sensitivity and stability, a conclusion could be made that mp-niobia-PE6200 is preferred as a sensitive building block of vapor responsive Bragg stacks.

We were interested to check and confirm whether the vapors penetrate the entire stack and reach the porous layer L2, which is the closest to the substrate. For this purpose, we ran three sets of fitting of transmittance spectra which was measured in acetone ambient in order to calculate Δn_{Ac} and estimate the fitting error in each fitting set. In the first minimization procedure, we only varied the refractive index of layer L6, which is the closest to the air. The dependence of the fitting error on calculated Δn_{Ac} is presented in Figure 7a. As we have already mentioned, the solution with the smallest fitting error is selected as a 'true' one. Using this criterion, the solution Δn_{Ac} = 0.105 is selected for the refractive index increase in layer L6, as it minimizes the fitting error (Figure 7c).

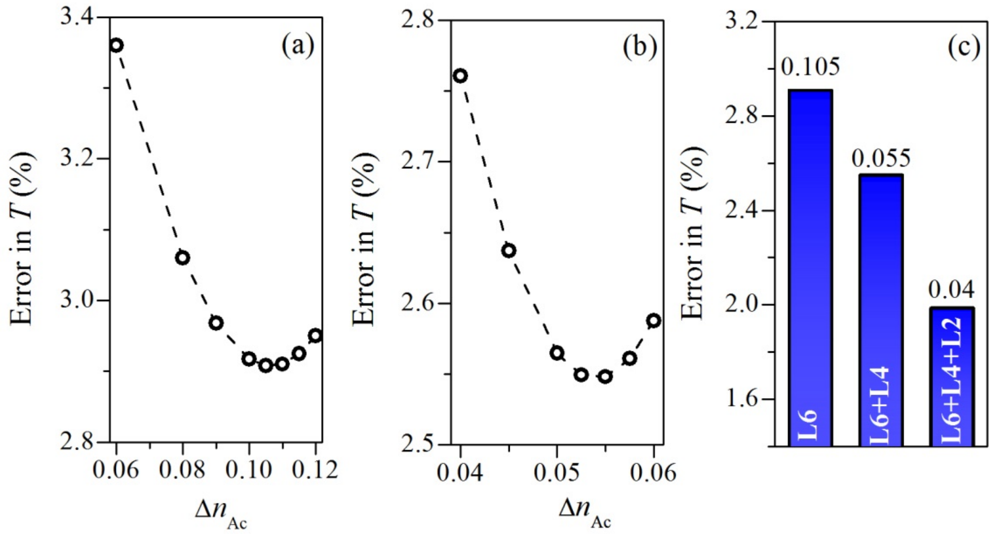

Figure 7. Dependence of fitting error on refractive index change Δn_{Ac} generated by acetone vapor condensation in layer L6, which is closest to the air (**a**) and in L6 and L4 layers (**b**); Fitting error values obtained when calculating Δn_{Ac} assuming vapor condensation in different porous layers in the stack denoted in the bars. The values indicate the calculated Δn_{Ac} ((**c**)).

In the next fitting step, refractive indices of both layers L6 and L4 are varied until the smallest error is reached. Thus, a value of 0.055 is obtained for Δn_{Ac}. The fitting error decreases in the first fitting set. The dependence error-versus-Δn_{Ac}, when all porous layers are considered, is already plotted in Figure 6b. From the comparison presented in Figure 7c, it is clear that the smallest fitting error, i.e., the best fit, is achieved when a contribution of all porous layers (L2 + L4 + L6) is considered. In this case, the calculated value for Δn_{Ac} is 0.04. That is in excellent agreement with previously obtained values concerning the refractive index response of single films [14].

In order to test the reproducibility and response time, the Bragg stack templated with PE6200 was subjected to cycles of sorption and desorption of acetone vapors and the results are given in Figure 8.

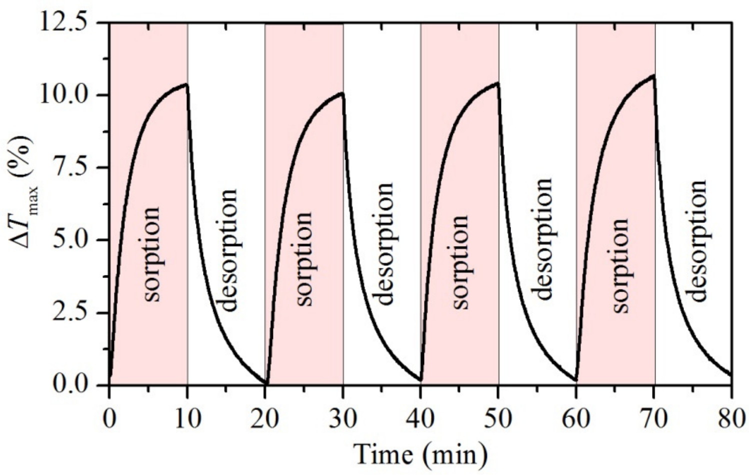

Figure 8. Sorption and desorption cycles of a 7-layer Bragg stack built from dense Nb_2O_5 films and mesoporous one templated with Pluronic PE6200. The relative pressure p/p_0 = 0.15 (p_0 pressure of saturated vapors at 0 °C).

In this experiment, the change in the transmittance of the Bragg stack at fixed wavelength ΔT_{max} is measured during alternation of acetone vapors and argon for an overall duration of 80 min. A very good reproducibility and stability of the structure response is observed. We should mention two considerable advantages: the stack operates at room temperature, and there is no need for additional heating for full analyte desorption.

The response time is longer when compared to single layer [14]: 50% of the maximum is reached in 88 s, and 80% in 213 s. However, we need to underline that the transmission change is more than 12 times stronger when a Bragg stack is used instead of a single film. In addition, the measurements performed in transmission mode are not only technologically easier to conduct but, also more precise.

3.5. Color Sensing

In order to prove the concept of color sensing of acetone vapors through measuring the transmittance of a Bragg stack, the color coordinates (CIE X иCIE Y) of the stack in transmission mode have been calculated before and during acetone exposure. As those parameters are linked to the sample color, their change could be correlated to the change in the sample color due to acetone adsorption. The color coordinates of the 7-layer stack templated with PE6200 are plotted in the CIE color space (Figure 9). It is seen that, although the two points are close to each other, they could be separated. Furthermore, even though the perceptual color difference is negligible to the naked eye, it could be detected by simple software compatible with devices such as smartphones or cameras.

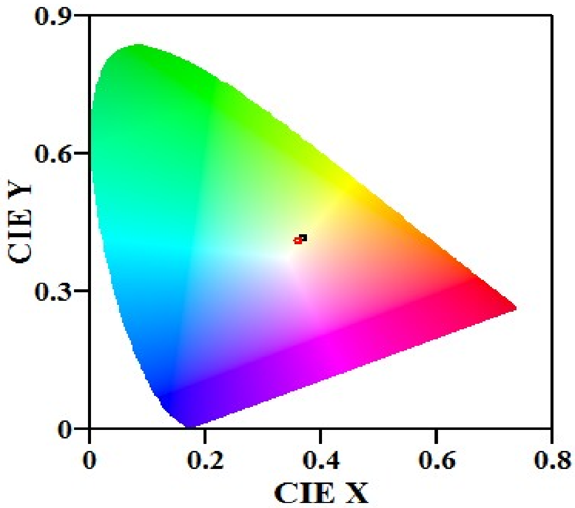

Figure 9. Color coordinates for a 7-layer Bragg stack built from dense Nb_2O_5 films and a mesoporous one templated with Pluronic PE6200 before (black dot) and during (red dot) exposure to acetone vapors.

4. Conclusions

Proper computer-aided design and successful deposition of all-niobia Bragg stacks utilized for optical sensing of VOC's through transmittance measurements were demonstrated. It was revealed that mesoporous films templated with Pluronic PE6200 (mp-niobia-PE6200) are more suitable for building blocks of vapor sensitive Bragg stacks compared to those prepared with PE6800 as an organic template. Due to lower porosity mp-niobia-PE6800 films exhibit a more rigid and stable skeleton, which more easily withstands the prolonged heat treatment applied during stacks deposition. In addition, it was demonstrated that vapor absorption and condensation in PE6200 templated Nb_2O_5 films is more effective than those in PE6800-tempated films, which was explained with the different film morphology: spherical pores in the latter case, and pores arranged in rows in the former. Very good reproducibility of the vapor response of all-niobia Bragg stacks templated with PE6200 was obtained. More than 12-times enhancement of sensitivity is achieved through the implementation of studied stacks as optical chemical sensors compared to the application of a single film. Furthermore, two considerable advantages are demonstrated: the sensing is performed at room temperature, and there is no need for additional heating for full analyte desorption. The additional option of color sensing is demonstrated which opens up the possibility of chemical sensing without the use of a power supply.

Author Contributions: Conceptualization, R.G. and T.B.; methodology, R.G. and T.B.; software, R.G. and T.B.; validation, R.G., B.G., and T.B.; formal analysis, R.G., Y.C., V.P., and B.G.; investigation, Y.C., V.P., and B.G.; resources, R.G.; data curation, R.G., Y.C., and V.P.; writing—original draft preparation, R.G. and T.B.; writing—review and editing, R.G., B.G., and T.B.; visualization, R.G., Y.C., V.P., and T.B.; supervision, R.G.; project administration, R.G.; funding acquisition, R.G. All authors have read and agreed to the published version of the manuscript.

Funding: This research was funded by Bulgarian National Science Fund (BNSF), grant number KP-06-M48/3 (26.11.2020).

Conflicts of Interest: The authors declare no conflict of interest. The funders had no role in the design of the study; in the collection, analyses, or interpretation of data; in the writing of the manuscript, or in the decision to publish the results.

References

1. Aguirre, C.I.; Reguera, E.; Stein, A. Tunable colors in opals and inverse opal photonic crystals. *Adv. Funct. Mater.* **2010**, *20*, 2565–2578. [CrossRef]
2. Zhao, Y.J.; Zhao, X.W.; Gu, Z.Z. Photonic crystals in bioassays. *Adv. Funct. Mater.* **2010**, *20*, 2970–2988. [CrossRef]
3. Zhao, Y.; Xie, Z.; Gu, H.; Zhu, C.; Gu, Z. Bio-Inspired variable structural color materials. *Chem. Soc. Rev.* **2012**, *41*, 3297–3317. [CrossRef] [PubMed]
4. Chiappini, A.; Tran, L.T.N.; Trejo-García, P.M.; Zur, L.; Lukowiak, A.; Ferrari, M.; Righini, G.C. Photonic crystal stimuli-responsive chromatic sensors: A short review. *Micromachines* **2020**, *11*, 290. [CrossRef]
5. Sang, L.; Vinu, A.; Coppens, M. Ordered mesoporous carbon with tunable, unusually large pore size and well-controlled particle morphology. *J. Mater. Chem.* **2011**, *21*, 7410–7417. [CrossRef]
6. Feng, P.; Bu, X.; Pine, D. Control of pore sizes in mesoporous silica templated by liquid crystals in block copolymer−cosurfactant−water systems. *Langmuir* **2000**, *5*, 5304–5310. [CrossRef]
7. Dai, F.; Zai, J.; Yi, R.; Mikhail, L.; Gordin, H.S.; Shuru, C.; Donghai, W. Bottom-Up synthesis of high surface area mesoporous crystalline silicon and evaluation of its hydrogen evolution performance. *Nat. Commun.* **2014**, *5*, 3605. [CrossRef] [PubMed]
8. Zhang, L.; Jin, L.; Liu, B.; He, J. Templated growth of crystalline mesoporous materials: From soft/hard templates to colloidal templates. *Front. Chem.* **2019**, *7*, 22. [CrossRef] [PubMed]
9. Guldin, S.; Kolle, M.; Stefik, M.; Langford, R.; Eder, D.; Wiesner, U.; Steiner, U. Tunable mesoporous bragg reflectors based on block-copolymer self-assembly. *Adv. Mater.* **2011**, *23*, 3664–3668. [CrossRef] [PubMed]
10. Griffith, K.J.; Forse, A.C.; Griffin, J.M.; Grey, C.P. High-Rate intercalation without nanostructuring in metastable Nb2O5 bronze phases. *J. Am. Chem. Soc.* **2016**, *138*, 8888–8899. [CrossRef] [PubMed]
11. Chen, D.; Wang, J.; Chou, T.; Zhao, B.; El-Sayed, M.; Liu, M. Unraveling the nature of anomalously fast energy storage in T-Nb_2O_5. *J. Am. Chem. Soc.* **2017**, *139*, 7071–7081. [CrossRef] [PubMed]
12. Khan, W.; Betzler, S.; Šipr, O.; Ciston, J.; Blaha, P.; Scheu, C.; Minar, J. Theoretical and experimental study on the optoelectronic properties of $Nb_3O_7(OH)$ and Nb_2O_5 photoelectrodes. *J. Phys. Chem. C* **2016**, *120*, 23329–23338. [CrossRef]
13. Georgiev, R.; Christova, D.; Todorova, L.; Georgieva, B.; Vasileva, M. Generating porosity in metal oxides thin films through introduction of polymer micelles. *Opt. Quant. Electron.* **2018**, *50*, 156. [CrossRef]
14. Georgiev, R.; Christova, D.; Georgieva, B.; Babeva, T. Organic framework engineering in mesoporous Nb_2O_5 thin films used as an active medium for organic vapors sensing. *Proc. SPIE* **2018**, *10691*, 1069128.
15. Lazarova, K.; Vasileva, M.; Marinov, G.; Babeva, T. Optical characterization of sol-gel derived Nb_2O_5 thin films. *Opt. Laser Technol.* **2014**, *58*, 114–118. [CrossRef]
16. Georgiev, R.; Georgieva, B.; Vasileva, M.; Ivanov, P.; Babeva, T. Optical properties of sol-gel Nb_2O_5 films with tunable porosity for sensing applications. *Adv. Condens. Matter Phys.* **2015**, *2015*, 403196. [CrossRef]
17. Lazarova, K.; Awala, H.; Thomas, S.; Vasileva, M.; Mintova, S.; Babeva, T. Vapor responsive one-dimensional photonic crystals from zeolite nanoparticles and metal oxide films for optical sensing. *Sensors* **2014**, *14*, 12207–12218. [CrossRef] [PubMed]
18. Georgiev, R.; Christova, D.; Todorova, L.; Georgieva, B.; Vasileva, M.; Novakov, C.; Babeva, T. Triblock copolymer micelles as templates for preparation of mesoporous niobia thin films. *J. Phys. Conf. Ser.* **2018**, *992*, 12037. [CrossRef]
19. Georgiev, R.; Lazarova, K.; Vasileva, M.; Babeva, T. All niobia Bragg stacks for optical sensing of vapors. *Opt. Quant. Electron.* **2020**, *2*, 114. [CrossRef]